Proceedings of the Sixth International Conference on Asian and Pacific Coasts (APAC 2011)
December 14 – 16, 2011, Hong Kong, China

INFLUENCE OF VELOCITY DISTRIBUTION AND DENSITY STRATIFICATION ON GENERATION OR PROPAGATION OF TSUNAMIS

T. KAKINUMA, K. NAKAMURA, K. YAMASHITA

Graduate School of Science and Engineering, Kagoshima University
1-21-40 Korimoto, Kagoshima, Kagoshima 890-0065, Japan

K. NAKAYAMA

Department of Civil and Environmental Engineering, Kitami Institute of Technology
165 Koen-cho, Kitami, Hokkaido 090-8507, Japan

A set of wave equations derived on the basis of a variational principle in consideration of both strong nonlinearity and strong dispersion of surface/internal waves is numerically solved to simulate generation and propagation of tsunamis in the vertical two-dimension. The velocity potential in each fluid layer is expanded into a power series of vertical position, such that the accuracy of vertical distribution of velocity depends on the number of expansion terms. Numerical results of surface displacement are compared with the existing experimental data, where tsunamis are generated by the seabed uplift. When the fundamental equations are reduced to nonlinear shallow water equations, the numerical model cannot represent propagation of a long wave group especially in distant-tsunami propagation, leading to overestimation of both the wave height and wave steepness of the first wave. The wave height becomes larger in the stratified ocean than that in a one-layer case, although the present density distribution hardly affects the tsunami phase over a long-distance travel.

1. Introduction

Numerical models based on shallow water equations, where the effects of both vertical distribution of horizontal velocity and vertical velocity are neglected, are usually used for calculation of tsunamis due to submarine earthquakes. Moreover, the effects of stratification in the ocean are not considered in tsunami simulation. In this study, nonlinear surface/internal wave equations derived through a variational principle [1] are numerically solved to evaluate these effects on generation or propagation of tsunamis. For example, Horrillo *et al*. [2] and Iwase [3] applied numerical models based on the Navier-Stokes and Boussinesq-type equations, respectively, to compare numerical results with those through shallow water models especially for distant-tsunami propagation. In the present study,

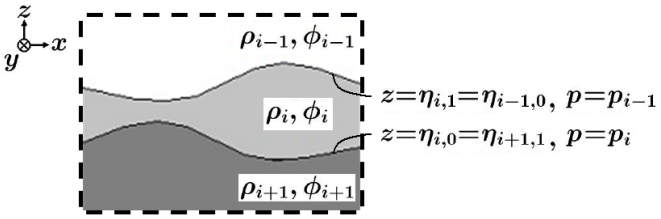

Figure 1. Mutilayer-fluid system.

the velocity potential is expanded into a power series on vertical position; then the dispersion, as well as the nonlinearity, of waves depends on the number of expansion terms of the velocity potential, i.e., the assumed vertical distribution of velocity. The numerical model tries to find solutions nearest to the true values based on the variational principle, such that the influence of velocity distribution on generation and propagation of tsunamis is studied by changing the number of expansion terms of the velocity potential.

Computation of tsunamis is performed in the vertical two-dimension. Surface displacements are compared between numerical results and the existing experimental data [4], where tsunamis are generated due to seabed uplift. Wave height and phase of tsunamis after a travel of a long distance are compared for various numbers of expansion terms of velocity potential. Tsunamis propagating over a continental slope or in two-layer water are also numerically simulated.

2. Governing Equations and Numerical Method

Inviscid and incompressible fluids, as shown in Fig. 1, are assumed to be stable in still water. The *i*-layer thickness in still water is denoted by $h_i(\boldsymbol{x})$. None of the fluids mix even in motion and the density ρ_i ($\rho_1 < \rho_2 < \ldots < \rho_I$) is spatially uniform and temporally constant in each layer. Surface tension and capillary action are neglected. Fluid motion is assumed to be irrotational, resulting in existence of velocity potential ϕ_i defined as $\boldsymbol{u}_i = \nabla\phi_i$ and $w_i = \partial\phi_i/\partial z$, where $\nabla = (\partial/\partial x, \partial/\partial y)$, i.e., a partial differential operator in the horizontal plane.

The pressure on $z = \eta_{i,0}$, i.e., the lower interface of the *i*-layer, is written by $p_i(\boldsymbol{x},t)$. In the *i*-layer, if both the elevation of one interface, $z = \eta_{i,1-j}(\boldsymbol{x},t)$ ($j = 0$ or 1), and the pressure on the other interface, $p_{i-j}(\boldsymbol{x},t)$, are known, then the unknown variables are the velocity potential $\phi_i(\boldsymbol{x},z,t)$ and interface elevation $\eta_{i,j}(\boldsymbol{x},t)$, such that the functional for the variational problem [1] is determined in the *i*-layer by

$$F_i[\phi_i, \eta_{i,j}] = \int_{t_0}^{t_1}\iint_A \int_{\eta_{i,0}}^{\eta_{i,1}} \left\{ \frac{\partial\phi_i}{\partial t} + \frac{1}{2}(\nabla\phi_i)^2 + \frac{1}{2}\left(\frac{\partial\phi_i}{\partial z}\right)^2 + gz + \frac{p_{i-j} + P_i}{\rho_i} \right\} dz\, dA\, dt, \qquad (1)$$

where $P_i = \sum_{k=1}^{i-1}(\rho_i - \rho_k)gh_k$; gravitational acceleration g is equal to 9.8 m/s^2.

The velocity potential ϕ_i is expanded into a power series of vertical position above the top face, i.e., the free surface, of still water, z, as

$$\phi_i(\boldsymbol{x},z,t) = \sum_{\alpha=0}^{N-1}\left\{ f_{i,\alpha}(\boldsymbol{x},t)\cdot z^{\alpha}\right\} \equiv f_{i,\alpha}z^{\alpha}. \tag{2}$$

We substitute Eq. (2) into Eq. (1), after which the functional F_i is integrated vertically; then the variational principle is applied to obtain Euler-Lagrange equations, that is the fully nonlinear equations for surface and internal waves.

If the number of water layers is equal to two, the equations are

[Upper layer] (i = 1)

$$\zeta^{\alpha}\frac{\partial\zeta}{\partial t} - \eta^{\alpha}\frac{\partial\eta}{\partial t} + \frac{1}{\alpha+\beta+1}\nabla\left\{\left(\zeta^{\alpha+\beta+1} - \eta^{\alpha+\beta+1}\right)\nabla f_{1,\beta}\right\} - \frac{\alpha\beta}{\alpha+\beta-1}\left(\zeta^{\alpha+\beta-1} - \eta^{\alpha+\beta-1}\right)f_{1,\beta} = 0, \tag{3}$$

$$\zeta^{\beta}\frac{\partial f_{1,\beta}}{\partial t} + \frac{1}{2}\zeta^{\beta+\gamma}\nabla f_{1,\beta}\nabla f_{1,\gamma} + \frac{1}{2}\beta\gamma\zeta^{\beta+\gamma-2}f_{1,\beta}f_{1,\gamma} + g\zeta = 0, \tag{4}$$

[Lower layer] (i = 2)

$$\eta^{\alpha}\frac{\partial\eta}{\partial t} - b^{\alpha}\frac{\partial b}{\partial t} + \frac{1}{\alpha+\beta+1}\nabla\left\{\left(\eta^{\alpha+\beta+1} - b^{\alpha+\beta+1}\right)\nabla f_{2,\beta}\right\} - \frac{\alpha\beta}{\alpha+\beta-1}\left(\eta^{\alpha+\beta-1} - b^{\alpha+\beta-1}\right)f_{2,\beta} = 0, \tag{5}$$

$$\begin{aligned}&\eta^{\beta}\frac{\partial f_{2,\beta}}{\partial t} + \frac{1}{2}\eta^{\beta+\gamma}\nabla f_{2,\beta}\nabla f_{2,\gamma} + \frac{1}{2}\beta\gamma\eta^{\beta+\gamma-2}f_{2,\beta}f_{2,\gamma} + g(\eta+h_1)\\ &-\frac{\rho_1}{\rho_2}\left\{\eta^{\beta}\frac{\partial f_{1,\beta}}{\partial t} + \frac{1}{2}\eta^{\beta+\gamma}\nabla f_{1,\beta}\nabla f_{1,\gamma} + \frac{1}{2}\beta\gamma\eta^{\beta+\gamma-2}f_{1,\beta}f_{1,\gamma} + g(\eta+h_1)\right\} = 0,\end{aligned} \tag{6}$$

where the surface, interface, and seabed are described by $z = \eta_{1,1} \equiv \zeta(\boldsymbol{x},t)$, $z = \eta_{1,0} = \eta_{2,1} \equiv \eta(\boldsymbol{x},t)$, and $z = \eta_{2,0} \equiv b(\boldsymbol{x},t)$, respectively.

In this paper, the seabed friction, fluid viscosity, and Coriolis force are not considered for simplicity. The governing equations are rewritten to a set of finite difference equations and the time development is carried out by applying implicit schemes similar to that of Nakayama and Kakinuma [5].

3. Influence of Velocity Distribution on Generation of Tsunamis

Numerical results of water surface displacement are compared with the experimental data [4] for verification of the present model. The area where $0\text{ m} \le x \le B_b = 0.305\text{ m}$ is raised touching a vertical wall at one end of the water basin of uniform width. The time variation of seabed position is given by $b + h_0 = b_0(1 - e^{-\varepsilon t})$ when $t > 0$. The initial water depth h_0 is equal to $B_b/12.2$; $b_0 / h_0 = 0.2$ and $t_c\sqrt{gh_0} / B_b = 0.069$, where $b + h_0 = 2b_0 / 3$ at $t = t_c$.

As shown in Fig. 2, the time variation of water surface displacement at the end where $x = 0$ m is well evaluated in comparison with the experimental data, as well as the three-dimensional calculation results [6], when the number of expansion terms of velocity potential shown in Eq. (2), i.e., N, is equal to three.

Numerical results of water surface displacement in the same case as that of

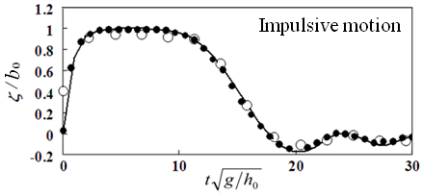

Figure 2. Water surface displacement ζ (x = 0 m; ○: experiment by Hammack [4], ●: three-dimensional numerical model [6], —: the present model, where N = 3).

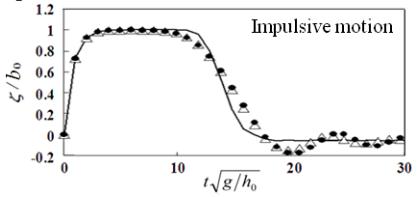

Figure 3. Water surface displacement ζ through the present model (x = 0 m; —: N = 1, △: N = 2, ●: N = 3).

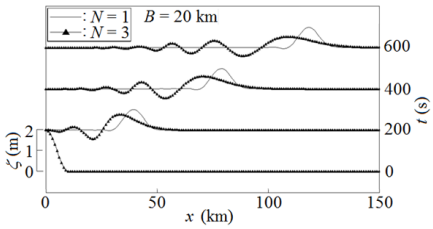

Figure 4. Water surface profile at each time (B = 20 km, N = 1 or 3).

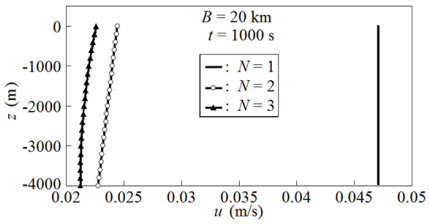

Figure 5. Horizontal velocity u below the first crest (B = 20 km, t = 1,000 s, N = 1,2, or 3).

Fig. 2 is shown in Fig. 3, according to which the shorter waves in the tsunami tail are not reproduced when N = 1, i.e., the set of governing equations is reduced to a set of nonlinear shallow water equations without wave dispersion. When N = 2, the model takes into account both linear and uniform vertical distributions of u_i and w_i, respectively, such that the balance between nonlinearity and dispersion is considered, leading to the more accurate result than that when N = 1. When N = 3, the effects of both parabolic vertical distribution of u_i and linear vertical distribution of w_i are also considered.

4. Influence of Velocity Distribution on Propagation of Tsunamis

In a calculation domain, the still water depth is equal to 4,000 m and a vertical wall exists at one end where x = 0 km. The initial water surface displacement is given by $\zeta(x,0) = a_0\{1+\cos[2\pi(x/B)]\}$ (0 km $\le x \le B/2$), where a_0 = 1.0 m and B means the initial wavelength.

Water surface profiles are shown in Fig. 4, where B = 20 km. When N = 1, both the front-surface slope and crest height of the first wave are larger without wave-group generation than those when N = 3, such that the peak time, i.e., the arrival time of the first crest, is too early when N = 1.

The vertical distribution of horizontal velocity u below the first crest is shown in Fig. 5, where $t=1{,}000$ s. When $N=1$, the horizontal velocity u is quite different from that when $N=2$ and 3. According to the present results, the

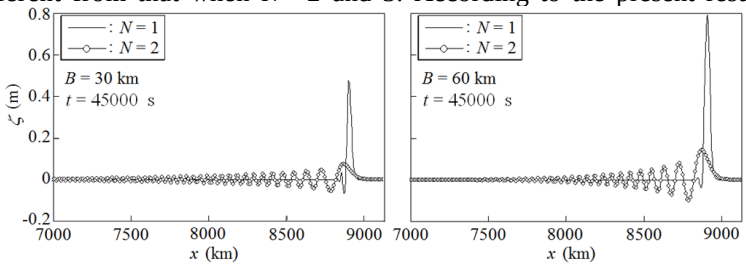

Figure 6. Water surface profile ($B=30$ or 60 km, $t=45{,}000$ s, $N=1$ or 2).

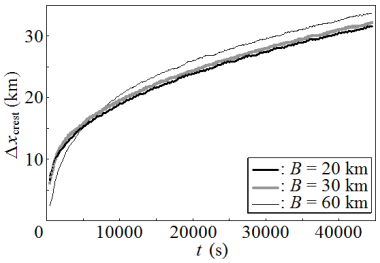

Figure 7. Horizontal distance of position between the first crests when $N=1$ and 2 ($B=20$, 30, or 60 km).

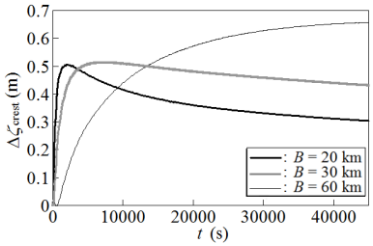

Figure 8. Difference of height between the first crests when $N=1$ and 2 ($B=20$, 30, or 60 km).

number of expansion terms of the velocity potential should be more than or equal to two in consideration of the balance between nonlinearity and dispersion of waves.

Water surface profiles are shown in Fig. 6, where $B=30$ and 60 km, $t=45{,}000$ s, and $N=1$ or 2. When $N=2$, the wave group consists of many waves; it should be noted that the shorter the initial wavelength B is, the longer the total length of the wave group is.

The horizontal distance of position, $\Delta x_{\mathrm{crest}}$, and the difference of height, $\Delta\zeta_{\mathrm{crest}}$, between the first crests when $N=1$ and 2 are shown in Figs. 7 and 8, respectively, where $B=20$, 30, or 60 km. According to Fig. 7, $\Delta x_{\mathrm{crest}}$ is more than 30 km when $t=45{,}000$ s. As shown in Fig. 8, the larger the initial wavelength B is, the larger the difference $\Delta\zeta_{\mathrm{crest}}$ is after $t=13{,}500$ s.

The wave height of the first wave, which includes the first crest and the first trough, H, and the horizontal distance between the first crest and the first trough, $x_{\mathrm{crest}}-x_{\mathrm{trough}}$, are shown in Figs. 9 and 10, respectively, where $B=20$, 30, or 60 km and $N=1$ or 2. According to these figures on the first wave, the wave steepness becomes larger as the initial wavelength is longer, i.e., the total initial

potential energy is larger. On the other hand, the wavelength does not depend on the initial wavelength but the propagating time.

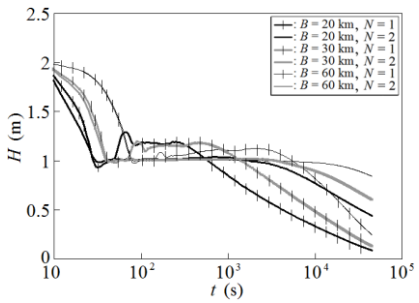

Figure 9. Wave height of the first wave (B = 20, 30, or 60 km, N = 1 or 2).

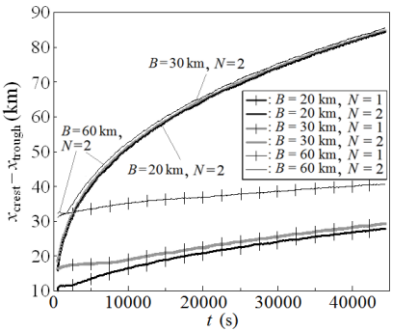

Figure 10. Horizontal distance between the first crest and the first trough (B = 20, 30, or 60 km, N = 1 or 2).

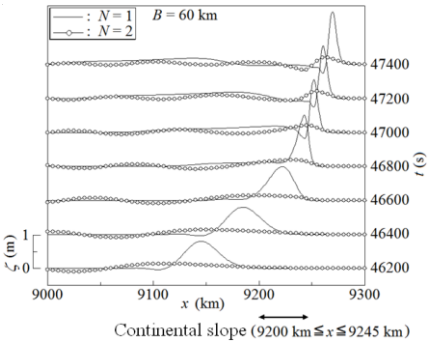

Figure 11. Water surface profile at each time (B = 60 km, N = 1 or 2).

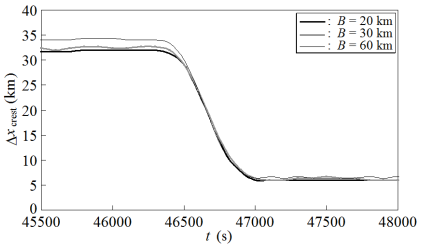

Figure 12. Horizontal distance of positions between the first crests when N = 1 and 2 (B = 20, 30, or 60 km).

5. Tsunamis Traveling over a Continental Slope

In a model of seabed configuration, it is assumed that two areas, where the still water depth is 4,000 and 200 m, are connected with a continental slope, the horizontal length of which is 45 km, and that the tsunami simulated inside the former area in **4.** continues propagation over the continental slope, where $9{,}200\ \text{km} \le x \le 9{,}245\ \text{km}$, and then the latter area, i.e., the continental shelf.

Water surface profiles are shown in Fig. 11, where B = 60 km and N = 1 and 2. The first wave, which has inclined backward due to wave dispersion over the flat seabed, begins to lean forward over the continental slope, increasing its wave height.

The horizontal distance between the first crests when $N=1$ and 2, i.e., Δx_{crest}, is shown in Fig. 12, where $B=20$, 30, or 60 km. In the present case, Δx_{crest}

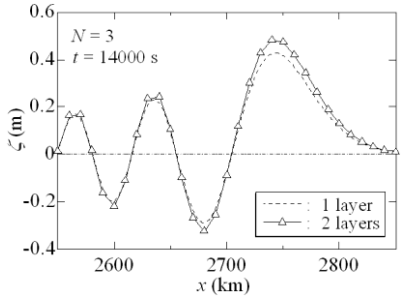

Figure 13. Water surface profile of tsunamis in one- or two-layer water (t = 14,000 s and $N=3$).

decreases to about 6 km over the continental slope, after that it is almost independent of the initial wavelength B over the continental shelf.

6. Influence of Density Stratification on Propagation of Tsunamis

It is assumed that the ocean where tsunamis propagate has uniform two-layer stratification over uniform seabed configuration to study the influence of density distribution on tsunami propagation. The still water depth is 150 and 3,850 m and the water density is 1020.26 and 1023.26 kg/m^3 in the upper and lower layers, respectively. On the other hand, in the case of one-layer water for comparison, the still water depth is 4,000 m. In these cases, a vertical wall is set at one end, where $x=0$ km, of the calculation domain and part of the seabed, where $0\,\text{km} \le x \le 15\,\text{km}$, is raised at a uniform upward velocity to the uplift height of 2 m within $0\,\text{s} \le t \le 20\,\text{s}$ to simulate tsunami generation and propagation in one- or two-layer ocean.

Water surface profiles are shown in Fig. 13, where $t=14{,}000$ s and $N=3$. According to the figure, the wave height of the first wave in the two-layer ocean is larger than that in the one-layer water by 13.4 %. The difference, however, of horizontal positions of the corresponding wave crests, as well as the wave troughs, between the one- and two-layer cases is practically nought, which means that even distant-tsunamis hardly feel the effect of density stratification.

7. Conclusions

The set of surface/internal wave equations derived on the basis of the variational principle was numerically solved to simulate generation and propagation of tsunamis in the vertical two-dimension. The velocity potential in each fluid layer was expanded into the power series on vertical position, such that the influence of velocity distribution on generation and propagation of tsunamis was studied by changing the number of expansion terms of the velocity potential.

According to the present results, the number of expansion terms of the velocity potential should be more than or equal to two, where both the horizontal and vertical velocities distributed linearly and uniformly, respectively, in the vertical direction are considered with the balance between nonlinearity and dispersion of waves; if the fundamental equations are reduced to nonlinear shallow water equations, then the numerical model has a disadvantage as follows:

(1) Shorter waves in a tsunami tail are not reproduced in the case where the velocity or acceleration of seabed uplift is larger.
(2) The tsunami height is too large and the wavelength is too short, leading to overestimation of the wave steepness.
(3) The peak time is too early but the error decreases during the tsunami propagation over a continental slope with forward inclination.
(4) A long wave group, which consists of many waves, is not represented especially in distant-tsunami propagation.
(5) The phenomenon where the wavelength of the first wave is independent of the initial wavelength after a long-distance travel does not appear.

The wave height becomes larger in the stratified ocean than that in the one-layer water, although the present density distribution hardly affects the distant-tsunami phase.

Acknowledgments

Sincere gratitude is extended to Prof. K. Fujima, National Defense Academy of Japan, for beneficial comments on propagation of tsunamis in stratified water.

This work was supported by Grant-in-Aid for Scientific Research (C) (21560544) of The Ministry of Education, Culture, Sports, Science, and Technology.

References

1. T. Kakinuma, Proc. 5th Int. Conf. on Computer Modelling of Seas and Coastal Regions, WIT Press, 225 (2001).
2. J. Horrillo, Z. Kowalik and Y. Shigihara, Marine Geodesy **29**, 149 (2006).
3. H. Iwase, Doctoral Dissertation, Tohoku Univ. (2005).
4. J. L. Hammack, J. Fluid Mech. **60**, 769 (1973).
5. K. Nakayama and T. Kakinuma, Int. J. Numer. Meth. Fluids **62**, 574 (2010).
6. T. Kakinuma and M. Akiyama, Proc. 30th Int. Conf. on Coastal Eng., ASCE, 1490 (2007).